AGU ADVANCING EARTH AND SPACE SCIENCE

JGR Atmospheres

RESEARCH ARTICLE
10.1029/2020JD033975

Key Points:

- Gas-phase hydrogen peroxide (H_2O_2) at the summit of Mt. Tai evidently increased from 2007 to 2018, which might be ascribed to volatile organic compounds (VOCs) increase and SO_2 decline
- Observed H_2O_2 at the foot of Mt. Tai could be well reproduced by a box model with H_2O_2 dry deposition velocity of 3 cm s^{-1} included
- O_3 formation in Tai'an city was mainly VOC-sensitive in the early morning and shifted to NO_x-sensitive thereafter

Supporting Information:

Supporting Information may be found in the online version of this article.

Correspondence to:

Y. Mu,
yjmu@rcees.ac.cn

Citation:

Ye, C., Xue, C., Zhang, C., Ma, Z., Liu, P., Zhang, Y., et al. (2021). Atmospheric hydrogen peroxide (H_2O_2) at the foot and summit of Mt. Tai: Variations, sources and sinks, and implications for ozone formation chemistry. *Journal of Geophysical Research: Atmospheres*, *126*, e2020JD033975. https://doi.org/10.1029/2020JD033975

Received 27 SEP 2020
Accepted 16 JUL 2021

Atmospheric Hydrogen Peroxide (H_2O_2) at the Foot and Summit of Mt. Tai: Variations, Sources and Sinks, and Implications for Ozone Formation Chemistry

Can Ye[1,2,3], Chaoyang Xue[1,2,4], Chenglong Zhang[1,2,5], Zhuobiao Ma[1,2], Pengfei Liu[1,2,5], Yuanyuan Zhang[1,2,5], Chengtang Liu[1,2,5], Xiaoxi Zhao[1,2], Wenjin Zhang[1,2], Xiaowei He[1,2], Yifei Song[1,2], Junfeng Liu[1,2,5], Weihao Wang[6], Benhui Sui[7], Ran Cui[7], Xue Yang[7], Rubo Mei[7], Jianmin Chen[8], and Yujing Mu[1,2,5]

[1]Research Centre for Eco-Environmental Sciences, Chinese Academy of Sciences, Beijing, China, [2]University of Chinese Academy of Sciences, Beijing, China, [3]Now at State Key Joint Laboratory of Environmental Simulation and Pollution Control, College of Environmental Sciences and Engineering, Peking University, Beijing, China, [4]Laboratoire de Physique et Chimie de l'Environnement et de l'Espace (LPC2E), CNRS, CNES, Université Orléans, Orléans, France, [5]Centre for Excellence in Regional Atmospheric Environment, Institute of Urban Environment, Chinese Academy of Sciences, Xiamen, China, [6]Department of Civil and Environmental Engineering, The Hong Kong Polytechnic University, Hong Kong, China, [7]Tai'an Municipal Ecological Environmental Bureau, Shandong Tai'an Ecological Environmental Monitoring Center, Tai'an, China, [8]Shanghai Key Laboratory Atmospheric Particle Pollution and Prevention (LAP3), Department of Environmental Science and Engineering, Institute of Atmospheric Sciences, Fudan University, Shanghai, China

Abstract Hydrogen peroxide (H_2O_2) acts as a terminal sink for atmospheric HO_x radicals (OH and HO_2), playing a key role in tropospheric O_3 formation. However, there are few field measurements of atmospheric H_2O_2 to assess its role in O_3 formation, especially for the seriously polluted region of the North China Plain. In this study, H_2O_2 concentrations were measured at the foot of Mt. Tai from May to July 2018 and the summit of Mt. Tai from May to June 2019, with average values of 0.93 ± 1.01 and 2.05 ± 1.20 ppb, respectively. H_2O_2 exhibited a pronounced diurnal variation with a noon-peak at the foot of Mt. Tai, which could be well reproduced by a gas-phase box model with H_2O_2 dry deposition velocity of 3 cm s^{-1} included, indicating H_2O_2 was mainly photochemically produced. Modeling analysis showed H_2O_2 production at the foot was most sensitive to alkenes and aromatics, while the source and sink for H_2O_2 were dominated by HO_2 recombination and dry deposition, respectively. Compared with the summer-measurement in 2007, the remarkable elevation of H_2O_2 at the summit might be ascribed to volatile organic compounds (VOCs) increase and SO_2 decline. Both H_2O_2-O_3 correlation and H_2O_2/NO_z ratio suggested O_3 formation at the foot of Mt. Tai was mainly VOC-sensitive in the early morning and shifted to NO_x-sensitive thereafter. Therefore, reduction of VOCs emission especially for the reactive species of alkenes and aromatics in the morning as well as NO_x emission around noontime will be effective for mitigating the serious O_3 (as well as H_2O_2) pollution in Tai'an city.

1. Introduction

Atmospheric hydrogen peroxide (H_2O_2) is mainly produced by recombination of two hydroperoxy radicals (HO_2) which involve the photochemical reactions of atmospheric VOCs and carbon monoxide (CO):

$$\mathrm{VOCs} + \mathrm{OH} \overset{O_2}{\rightarrow} \mathrm{RO_2} + \mathrm{H_2O} \tag{R1}$$

$$\mathrm{RO_2} + \mathrm{NO} \overset{O_2}{\rightarrow} \mathrm{OVOC} + \mathrm{HO_2} + \mathrm{NO_2} \tag{R2}$$

$$\mathrm{CO} + \mathrm{OH} \overset{O_2}{\rightarrow} \mathrm{CO_2} + \mathrm{HO_2} \tag{R3}$$

$$HO_2 + HO_2 \rightarrow H_2O_2 + O_2 \tag{R4}$$

H_2O_2 formation through R4 is easily suppressed by the presence of nitric oxide (NO) because the reaction rate constant (8.8×10^{-12} cm^3 $molecule^{-1}$ s^{-1}) of R5 is nearly five times greater than that (1.5×10^{-12} cm^3 $molecule^{-1}$ s^{-1}) of R4 at 298 K (Sander et al., 2003).

$$HO_2 + NO \rightarrow OH + NO_2 \tag{R5}$$

Theoretically, H_2O_2 formation through R4 will be negligible when NO levels exceed 1 ppbv, which is also supported by most field observations (Hua et al., 2008; Nunnermacker et al., 2008; Walker et al., 2006; Watanabe et al., 2016). Besides H_2O_2 formation through R4, ozonolysis of unsaturated VOCs has been identified as another source of H_2O_2, which is usually considered to be the dominant source of H_2O_2 in nighttime (Becker et al., 1990, 1993). Furthermore, the photochemical reactions in liquid-phase, such as cloud, fog, and atmospheric particles, can also produce H_2O_2 (Anastasio et al., 1994; Faust et al., 1993; Herrmann et al., 2015; Zuo & Hoigné, 1993). The atmospheric hydroxyl radicals (OH) and HO_2 can be recycled through R1–R3 and R5, whereas H_2O_2 formation through R4 terminates the circle of HO_x radicals (OH and HO_2) because reproduction of OH radicals via H_2O_2 photolysis (R6) in the troposphere is very slow.

$$H_2O_2 + h\nu\left(\lambda \le 360\ \mathrm{nm}\right) \rightarrow 2OH \tag{R6}$$

H_2O_2 formation through R4 usually acts as the dominant sink for HO_x radicals under the condition with low NO levels or high $VOCs/NO_x$ (NO and NO_2) ratios. Under the condition with relatively high NO levels or low $VOCs/NO_x$ ratios, however, the termination of HO_x radicals is usually dominated by the reaction of NO_2 with OH (Tan et al., 2018):

$$NO_2 + OH \rightarrow HNO_3 \tag{R7}$$

When H_2O_2 formation through R4 acts as the dominant sink for HO_x radicals, more NO_x will accelerate the conversion rate of NO to NO_2 through R2 and R5 leading to more O_3 formation via photolysis of NO_2, whereas additional VOCs will lead negligible influence on O_3 because of the limited NO_x levels. When HNO_3 formation through R7 acts as the dominant sink for atmospheric HO_x radicals, however, increase of NO_x will suppress O_3 formation due to titration reaction of O_3 by NO, while increase of VOCs will accelerate O_3 formation by promoting the conversion rate of NO to NO_2 because more OH radicals will react with VOCs through R1 to compete with R7. Therefore, the H_2O_2/HNO_3 ratio is a good indicator for judging the relative roles of H_2O_2 and HNO_3 in termination of HO_x radicals and for assessment of the VOCs-NO_x-O_3 sensitivity (Hammer et al., 2002; Peng et al., 2006; Sillman, 1995; Sillman et al., 1998). Additionally, H_2O_2 also play a dominant role in sulfate formation through liquid-phase oxidation of sulfur dioxide (SO_2) in clouds, fogs, and deliquescent particles to account for acid deposition as well as deterioration of regional air quality (Calvert et al., 1985; Penkett et al., 1979; Shen et al., 2012; Ye et al., 2018). A recent study pointed out that the SO_2 oxidation rate by H_2O_2 can be greatly enhanced in deliquesced aerosols with high solute strengths in comparison with dilute bulk aqueous solutions (T. Liu et al., 2020). Furthermore, H_2O_2 can pass into leaves or the human body to form liquid-phase free radical species (i.e., OH and HO_2) for attacking nucleic acids and proteins leading to cell damage (Möller, 1989; Tao et al., 2003).

Considering the important roles of H_2O_2 in tropospheric chemistry as well as its adverse impact on the ecosystem, a growing number of measurements for atmospheric H_2O_2 have been reported in different places, including urban, rural and mountain sites as well as airborne measurements (Gong et al., 2018; Lee et al., 1997; Liang et al., 2013; Tanner & Schorran, 1995; Walker et al., 2006; Wang et al., 2016; Watanabe et al., 2016; Zhang et al., 2018). In general, relatively high H_2O_2 levels (from several ppb to more than 10 ppb) usually occur in polluted regions or pollution plumes, for example, H_2O_2 mixing ratio up to 11.3 ppb was observed in a seriously polluted rural site in China (Wang et al., 2016) and 11.5 ppb in pollution plumes during flights in the marine troposphere (O'Sullivan et al., 1999). Photochemical pollution is severe in China especially in the North China Plain (NCP) and the surface O_3 level has been found to exhibit a significant increasing trend of 1–2 ppb yr^{-1}due to high anthropogenic emissions (Sun et al., 2016; Zhang et al., 2014). To our knowledge, H_2O_2 field measurements and analysis of H_2O_2 photochemistry in China are still scarce and thus urgently needed for a better understanding of tropospheric chemistry and O_3 sensitivity to NO_x or VOC emissions.

In this study, simultaneous observation of H_2O_2 and other relevant pollutants were performed at the foot of Mt. Tai in the summer of 2018 and at the summit of Mt. Tai in the summer of 2019 to explore H_2O_2 levels, variation characteristics and influencing factors. Based on the observational data measured at the foot of Mt. Tai, a zero-dimensional box model was employed to simulate the H_2O_2 budget. Additionally, H_2O_2-O_3 correlation and the ratios of H_2O_2/NO_z (the sum of reactive nitrogen compounds except for NO_x) were used to evaluate the VOCs-NO_x-O_3 sensitivity.

2. Materials and Methods

2.1. Field Study Site

The mountain measurement was conducted at the Meteorological Observatory located at the summit of Mt. Tai (36.25°N, 117.10°E, 1,534 m a.s.l-above sea level, Figure S1) in Shandong province, China. Mt. Tai is located at the center of NCP. It is 15 and 30 km away from the Tai'an and Jinan city (the capital city of Shandong province), respectively. The altitude of the site is near the top of the boundary layer during the daytime in summer and in the residual layer at night. Studies have been conducted at this site to study cloud and particle chemistry and gas pollutants (Kanaya et al., 2013; Shen et al., 2012; Sun et al., 2016). This mountain site is thought to experience few local emission sources and provide regionally representative data for the NCP. The measurements took place from May to June in 2019.

The ground measurement took place from May to July 2018 at an urban site which located in Electric Power College in Tai'an City (36.18°N, 117.11°E), about 10 km away from the foot of Mt. Tai. Tai'an city is located in central Shandong province at the eastern edge of the NCP, between the Bohai Economic Rim and Yangtze River Delta Economic Zone. Tai'an has a population of 15 million citizens. Recent years Tai'an city experiences serious O_3 pollution in summer season.

2.2. Instrumentation

H_2O_2 was measured by a commercial monitor (AL2021, Aerolaser, Germany) based on wet chemical dual enzyme detection technique described by Lazrus et al. (1986). Gaseous H_2O_2 is sampled in buffered solution (pH = 5.8–6.0) in a glass stripping coil. Soluble organic peroxides can also dissolve into the stripping solution. After sampled by the stripping coil, the peroxides solution is divided into two channels and then reacts with *p*-hydroxyphenyl acetic acid (POPHA) and horseradish peroxidase. The reaction yields fluorescent dye which can be measured via fluorescence spectroscopy. Since all soluble peroxides can be detected by the reaction, one channel was added catalase prior to the reaction with POPHA in order to selectively destroy H_2O_2. The signal difference between the two channels represents the H_2O_2 concentrations. During the field campaigns, the liquid calibration was performed every 1 or 2 days with liquid H_2O_2 standards (33.3 $\mu g\ L^{-1}$). The detection limit of the instrument is lower than 50 pptv with noise <2% at full scale and has an uncertainty of 10% (Fischer et al., 2015; Ye et al., 2018). The 1-min averages were recorded by a data logger. In this article, hourly averages were reported.

Measurements of HONO were conducted by a commercial LOPAP instrument (Long path absorption photometer, QUMA, Germany) which works based on a wet chemical technique (Heland et al., 2001). To avoid potential interferences induced by long inlet lines and heterogeneous or loss of HONO, HONO sampling unit was installed directly in the outdoor atmosphere. LOPAP collects HONO in stripping coil and then converts it into a dye which is detected using long path absorption. The instrument has two stripping coils placed in series to reduce known interfering signals.

A total of 56 non-methane hydrocarbons (NMHCs) were measured continuously and automatically using a liquid-nitrogen-free GC-FID instrument, with a time resolution of 1 h. Detailed information about the GC-FID can be found in C. Liu et al. (2016). The oxygenated volatile organic compounds (OVOCs) were sampled by adsorption-reaction cartridges with time resolution of 2 h, and then analyzed by high liquid chromatography (HPLC) method. Air sample passed through an ozone scrubber and a Sep-Pak DNPH-Silica Cartridge

Table 1
Comparison of the Observed Parameters at the Foot and Summit of Mt. Tai

Parameters	Ground site	Mountain site
Temperature (°C)	27.68 ± 3.73	16.20 ± 3.35
RH (%)	49.46 ± 17.79	58.98 ± 18.19
Wind speed (m s^{-1})	1.93 ± 0.97	6.34 ± 3.85
NO (ppb)	1.88 ± 6.96	0.64 ± 0.10
NO_2 (ppb)	14.49 ± 9.59	3.02 ± 1.33
O_3 (ppb)	58.28 ± 30.46	74.53 ± 12.06
SO_2 (ppb)	3.42 ± 3.82	1.23 ± 0.66
$PM_{2.5}$ (ppb)	30.94 ± 12.45	29.12 ± 19.28
CO (ppb)	263.1 ± 230.6	271.2 ± 113.2
H_2O_2 (ppb)	0.93 ± 1.01	2.05 ± 1.20

and carbonyl compounds were trapped by cartridges. After sampling, the cartridges were brought to lab for elution using acetonitrile as eluent. The eluent solution was then injected in HPLC for analysis.

Trace gases including NO, NO_2, SO_2, O_3, and CO were measured by a series of online monitors. NO and NO_2 were measured with the commercial Thermo Model 42i analyzer based on chemiluminescence technique. SO_2 was measured by Thermo Model 43i using pulsed UV fluorescence. O_3 measurements were performed based on UV absorption by the commercial Thermo 49i. Thermo 48i was used to measure CO. Multipoint calibration and zero and span checks were performed every week to ensure the data accuracy. Meteorological measurements (e.g., temperature, pressure, wind speed and direction, relative humidity, and solar radiation) were available from a potable weather station (Model WXT520, Vaisala, Finland) installed on the roof of a six-story teaching building near the sampling site.

2.3. Box Model Setup

A zero-dimensional box model using a near-explicit mechanism, MCM (Master Chemical Mechanism) Version 3.3.1 (Sommariva et al., 2020) was employed to examine the budget of atmospheric H_2O_2. The model treated the air pollutants to be well-mixed within the boundary layer and did not consider the dilution and transport. Simulations were only performed for the ground site due to the fact that the mountain site is greatly influenced by mountain-valley breeze, regional transport, and long-range transport (Kanaya et al., 2013; Ren et al., 2009) which could not be considered by the box model. MCMv3.3.1 describes the degradation of 143 VOCs with about 5,800 species and 17,000 reactions and has been extensively used in past studies of photochemistry. In our study, measurements of NO, NO_2, O_3, CO, NMHCs, OVOCs, HONO, H_2O, temperature, pressure, and $j(NO_2)$ were used as inputs to constrain the model calculations. The model ran with a 1-h time step and a spin-up time of 2 days to reach a steady state. The boundary layer height was derived from the HYSPLIT model and varied between 1,500 m in daytime to 500 m in nighttime. Dry deposition loss in the box model was expressed as dry deposition velocity divided by boundary layer height.

3. Results and Discussion

3.1. Meteorological and Chemical Conditions

Figure S2 illustrated the time series of H_2O_2 and relevant parameters for the entire observation period at the foot of Mt. Tai. The comparison of observed parameters for both sites is shown in Table 1. The meteorological conditions at the foot of Mt. Tai during the observation period was characterized by high temperature (average: 27°C; max: 37°C), high relative humidity (average: 49%; max: 90%) and strong solar radiation (up to 800 W m^{-2}), which favored the production of photochemical oxidants. The wind speeds were usually below 2 m s^{-1}. Most of the days were sunny with exceptions of few rainy days (9 June, 25–26 June). During these rainy days, the maximum O_3 concentrations were below 60 ppb. The back trajectory cluster analysis by HYSPLIT4 model (NOAA, USA, http://ready.arl.noaa.gov/HYSPLIT.php) showed that air mass arriving at the measurement site mainly came from the Shandong Peninsula and southern areas of Shandong province with large emissions of air pollutants (Figure S3). Relatively low NO levels during the whole period will be beneficial to the accumulation of O_3 and H_2O_2. As shown in Figure S2, O_3 hourly averaged levels frequently exceeded the Class-2 limit values (160 μg m^{-3} which is equivalent to 82 ppb at 25°C and 1,013 kPa) of National Ambient Air Quality Standard of China (GB3095-2012), implying severe photochemical O_3 pollution during summer season at Tai'an city. The particulate pollution was not severe with average concentrations of 30.9 μg m^{-3}.

For the mountain site, the temperature during the observation period was much lower (average: 16.2°C) than that at the ground site. The relative humidity was high with an average value of 59% as clouds and fog events occurred frequently at the mountain site in summer. High wind speed prevailed which suggested the

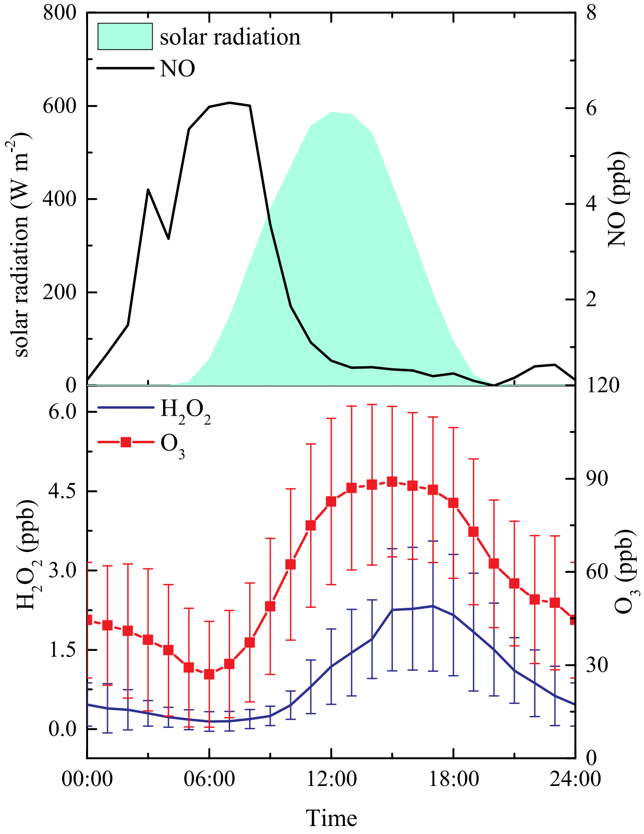

Figure 1. Average diurnal patterns for mixing ratios of H_2O_2, O_3, NO, and solar radiation at the foot of Mt. Tai. The vertical bars show standard errors for H_2O_2 and O_3.

site is easily influenced by transportation. Back trajectory cluster analysis showed air flow from Shandong Peninsula and southern areas where large city clusters are located dominated the air mass transport to the summit of Mt. Tai (Figure S3). This transport patterns are mainly driven by summer Asian monsoon (Ding et al., 2008; Sun et al., 2016). As Mt Tai is the highest mountain in the center of NCP and the summit is within the planetary boundary layer during daytime, the high-elevation site is regionally representative of the NCP where it is suffering from severe photochemical pollution during summer season. The average concentrations of primary pollutants NO (0.6 ppb), NO_2 (3.0 ppb), and SO_2 (1.2 ppb) at the summit were lower than those at the ground site, which were 1.8 ppb for NO, 14.4 ppb for NO_2, and 3.4 ppb for SO_2. CO (271 ppb vs. 263 ppb) and $PM_{2.5}$ (29.1 μg m^{-3} vs. 30.9 μg m^{-3}) were comparable at the two sites (Table 1).

3.2. Diurnal Variations

Obviously, a distinct H_2O_2 peak could be observed in each day at the foot of Mt. Tai, which was in line with the diurnal profiles of O_3 and solar radiation (Figure S2). To clearly exhibit the relationship among H_2O_2, O_3, NO, and solar radiation at the foot of Mt. Tai, their average diurnal variations are shown in Figure 1. The evident increase of both H_2O_2 and O_3 mixing ratios from the morning to the afternoon verified that they were mainly from daytime photochemical reactions (Figure 1). Both H_2O_2 and O_3 formations are directly related to the reactions of HO_2 radicals which are formed by photolysis of carbonyls and the photooxidation of VOCs and CO initiated by OH radicals (R1–R3), resulting in their similar daytime increasing trends. Due to the effective suppression of H_2O_2 formation by NO (R5) in the early morning, growth of H_2O_2 mixing ratio commenced around 9:00 when NO concentration was less than 1 ppb, whereas a steep increase of O_3 concentration occurred just after sunrise (around 6:00) when NO concentration was the highest (more than 6 ppb). In the morning, O_3 formation is generally in the NO_x-saturated regime. When NO_x began to decrease (time when NO was the highest), radical scavenging by NO_x oxidation to HNO_3 weakened which led to more O_3 production.

As solar radiation is the key precondition for triggering atmospheric photochemical reactions, the minimal H_2O_2 peak values (~0.5 ppb) were observed on cloudy days (e.g., on 13 July) with weak solar radiation. Besides solar radiation, other factors also played important roles in H_2O_2 formation. For example, the H_2O_2 peak values varied from ~2 to 6 ppb on the clear days with approximately the same solar radiation intensity, which was suspected to relate with the daily variations of NO_x, VOCs, CO, and the precursors of OH radicals that will be validated by the box model calculations constrained by the observational data in the following section. Although the uptake of H_2O_2 by particles during dust event has been proposed (de Reus et al., 2005; Qin et al., 2018), relatively high daytime H_2O_2 peak values (>2 ppb) were usually observed on the days when $PM_{2.5}$ concentrations were higher than 40 μg m^{-3}, indicating that the promotion effect on H_2O_2 formation due to increase of VOCs, CO and OH precursors with the accumulation of $PM_{2.5}$ greatly exceeded the H_2O_2 suppression effect by the $PM_{2.5}$.

After reaching its maximum around 17:00, H_2O_2 started to decrease and maintained low concentrations (around the detection limit) throughout the night due to fast dry deposition loss. O_3 concentrations also decreased in the late afternoon and frequently maintained high levels during the night (e.g., 3–8 June) which might be explained by lower dry deposition velocity than that of H_2O_2 (Crowley et al., 2018).

Figure 2 shows the average diurnal patterns of H_2O_2 and O_3 observed at the summit of Mt. Tai. Time series of H_2O_2 and O_3 were depicted in Figure S4. The H_2O_2 at the summit of Mt. Tai were highly variable with daily concentrations changing notably during the study period (Figure S4). This phenomenon could be explained by the influence of mountain-valley breeze and cloud scavenging. H_2O_2 has a high Henry Law constant

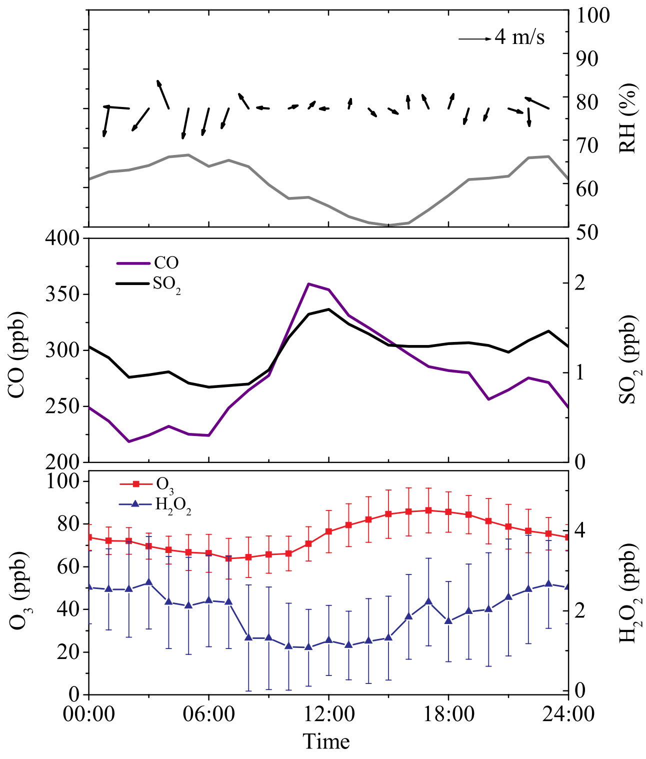

Figure 2. Average diurnal patterns of H_2O_2, O_3, CO, SO_2, relative humidity (RH), wind speed, and direction measured at the summit of Mt. Tai.

(1×10^5 M atm^{-1}) and hence is readily soluble in the liquid-phase. Consequently, gas-phase H_2O_2 concentrations are influenced by cloud and fog events. For example, during nighttime on 5 June (Figure S4), a sharp decrease of H_2O_2 coincided with an evident elevation of RH (up to 90%), suggesting the uptake of H_2O_2 by cloud or fog droplets. Previous studies have reported high H_2O_2 concentrations in the cloud samples at the summit of Mt. Tai (Li et al., 2020; Shen et al., 2012), which mainly came from the wet removal of gas-phase H_2O_2. Assuming the H_2O_2 concentrations in cloud and Henry Law constant are 45.1 μM (average value measured by Li et al. [2020]) and 1×10^5 M atm^{-1}, respectively, then the gas-phase H_2O_2 concentrations are estimated to be 0.4 ppb, which is similar to the levels measured during the cloud event on 5 June. The high H_2O_2 detected in the cloud could also indicate high gas-phase H_2O_2 at the summit of Mt. Tai. It can be clearly seen that, from the average diurnal pattern in Figure 2, H_2O_2 exhibited a broad minimum in daytime and then increased to maximum until midnight, which was a typical pattern observed at mountain sites (Balasubramanian & Husain, 1997; Fischer et al., 2019; Ren et al., 2009). Obvious enhancements of primary pollutants (CO and SO_2) could be clearly seen after 6:00, which suggested the influence of upslope mountain-valley breeze and convective mixing. Additionally, the change of wind vector after 6:00 also indicated vertical transport by southerly and southwesterly airflows along the slope of the mountain. Therefore, the H_2O_2 and O_3 increased during daytime, a process not only influenced by photochemical production but also upward transport from the foot of Mt. Tai by the mountain-valley breeze. Consistent phenomenon was also observed at the summit of Mt. Tai by previous studies (Cui et al., 2020; Gao et al., 2005; Ren et al., 2009). The increase lasted to the evening and then the concentrations of O_3 and H_2O_2 remained nearly constant during the night. As the sampling site was in the residual layer at night, the dry deposition loss was minimized. In the early morning, with the development of the mixed layer, the mixing of H_2O_2 lead to a sharp drop of H_2O_2 concentrations at the high-elevation site.

Although the two measurements were both conducted in summer seasons, these measurements were done in different periods and different years, making it difficult to directly do comparison between the two sites. Nevertheless, we could have a preliminary analysis. As mentioned earlier, concentrations of primary pollutants at the summit were typically lower or comparable than those at the ground site, while the average concentrations of secondary pollutants like H_2O_2 and O_3 were higher at the summit than at the foot of Mt. Tai (Table 1). This phenomenon of higher H_2O_2 and O_3 concentrations at the summit could be explained by two possible reasons: the dry deposition loss and other sinks were minimized at the high-elevation site as the site was in the residual layer during the night and hence high night concentrations were preserved; in addition, H_2O_2 and O_3 concentrations at the summit were greatly affected by regional transport from NCP areas, where are suffering from severe photochemical pollution in summer season.

3.3. Comparison With Previous Studies

In Table 2 we compare our observed H_2O_2 concentrations with those measured at ground and mountain sites in previous studies. Only summer data was summarized. For the measurements at ground level, the mean H_2O_2 concentration of 0.93 ppb in the small city of Tai'an was evidently higher than those of the megacity of Beijing (0.20 ppb), Wangdu (0.51 ppb, a rural site in center of the Beijing-Tianjin-Hebei region), Southeastern tip of Hong Kong Island (0.29 ppb), Korea University (0.81 ppb), and Hyytiälä, Finland (0.382 ppb), but lower than that (1.26 ppb) of the megacity of Guangzhou. The lowest mean H_2O_2 concentration in Beijing city was probably ascribed to relatively high NO_x concentrations which suppressed H_2O_2 formation, and the highest value in Guangzhou might be attributed to higher VOCs emissions especially for highly reactive biogenic VOCs because of high vegetation coverage, relatively high solar radiation intensity and temperature in the subtropical area. Although the latitude of the southeastern tip of Hong Kong Island

Table 2
Summary of Some Gas-Phase H_2O_2 Measurements at Ground and Mountain Sites in Previous Studies

	Measurement site	Altitude (m)	Period	H_2O_2 concentration (ppbv)	References
Ground sites	Zion Supersite (42.47°N, 87.81°W)	160	June 1–23, 2017	0.5–8 (daytime)	Vermeuel et al. (2019)
	Korea University (37.35°N, 127.01°E)	90	June–August 2003	Mean: 0.81 (0.21–1.61)	Lee et al. (2008)
	University of Nevada (39.55°N, 119.82°W)	10	June–December 1999	0.012–2.74	J. Liu et al. (2003)
	Hyytiälä, Finland (61.50°N, 24.17°E)	181	July 12–August 12, 2010	0.382 (0.209–0.786)	Fischer et al. (2019)
	Southeastern tip of Hong Kong Island (22.21°N, 114.25°E)	60	May 9–June 13, 2011	0.29 ± 0.16	Guo et al. (2014)
	Wangdu (38.66°N, 115.25°E)	35	June 4–July 7, 2014	Mean: 0.51 (0.01–11.3)	Wang et al. (2016)
	Beijing (39.99°N, 116.30°E)	53	August 2010	0.20 ± 0.28 maximum: 1.59	Liang et al. (2013)
	Guangzhou (23.54°N, 113.06°E)	36	July 18–30, 2006	1.26 ± 1.24 (daytime) maximum: 4.6	Hua et al. (2008)
	Taian city (36.18°N, 117.11°E)	86	May 30–July 13, 2018	0.93 ± 1.01 (0.1–6.06)	This study
Mountain sites	Mt. Mitchell (35.76°N, 82.26°W)	2,006	July–August 1988	Mean: 0.76 maximum: 4.18	Claiborn and Aneja (1991)
	Mt. Norikura (36.10°N, 137.55°E)	2,770	July–September 1993	0.1–4.5	Watanabe et al. (1995)
	Mt. Whiteface (43.93°N, 71.40°W)	1,483	July 1995	1.5–5.15	Balasubramanian and Husain (1997)
	Sky Forest, San Bernardino Mountains (34.12°N, 116.87°W)	1,790	Spring through fall 1987–1990	0.79–3.25	Sakugawa and Kaplan (1993)
	Mt. Tai (36.26°N, 117.11°E)	1,534	June–July 2007	0.55 ± 0.67	Ren et al. (2009)
	Mt. Tai (36.26°N, 117.11°E)	1,534	May–June 2019	2.05 ± 1.20 (0.05–5.36)	This study

is very close to Guangzhou city, the mean H_2O_2 concentration at the island was only one-fourth of that in Guangzhou city, further revealing that the photochemical processes in polluted areas are important sources for atmospheric H_2O_2. The mean H_2O_2 concentration at the foot of Mt. Tai was the highest among those measured at the places in the middle latitudes (36°–40°N), implying that the combined air pollution from anthropogenic and biogenic emissions might be in favor of H_2O_2 formation. The maximal daytime H_2O_2 value of 6.06 ppb at the foot of Mt. Tai was at least a factor of 2 larger than those measured at various sampling sites, but lower than those measured in Zion Supersite (8 ppb) and Wangdu (11.3 ppb).

For the mountain measurements with altitudes ranging from 1,483 to 2,770 m, the mean H_2O_2 concentration (2.05 ppb) and maximal H_2O_2 concentration (5.36 ppb) measured at the summit of Mt. Tai in our study was the highest among those reported in the literature. For the same sampling site at the summit of Mt. Tai, the mean H_2O_2 concentration measured by this study was about a factor of 3 greater than that measured during the period of June–July in 2007. Zhou et al. (2019) found that tropospheric column HCHO from satellite observations, which is indicative of the change of reactive VOCs, showed an increase of 0.05×10^{15} molecules cm^{-2} yr^{-1} during the whole period from 2005 to 2016 in the NCP. Therefore, the remarkable increase of H_2O_2 from 2007 to 2019 at the summit of Mt. Tai might be ascribed to the increase of VOCs emissions. Moreover, since China launched the toughest-ever clean air action plan to resolve serious pollution issues in 2013, SO_2 concentrations in 2017 decreased by 66% compared to the 2013 level in Beijing-Tianjin-Hebei area, which resulted in a 49% reduction in sulfate concentrations (Geng et al., 2019). H_2O_2 is one of the most important oxidants for liquid-phase SO_2 oxidation and hence SO_2 reduction would lead to less H_2O_2 consumption, especially for the mountain site where the clouds events frequently occur. A recent study reported an increasing trend of H_2O_2 concentrations in the cloud samples at the summit of Mt. Tai from 2014 to 2018 (Li et al., 2020), which suggested less SO_2 consumption of H_2O_2 and the increase of gas-phase H_2O_2 concentrations at a certain degree. Therefore, both VOCs increase and SO_2 reductions are the potential driving factors leading to much higher gas-phase H_2O_2 concentrations than 10 years ago at the summit of Mt. Tai.

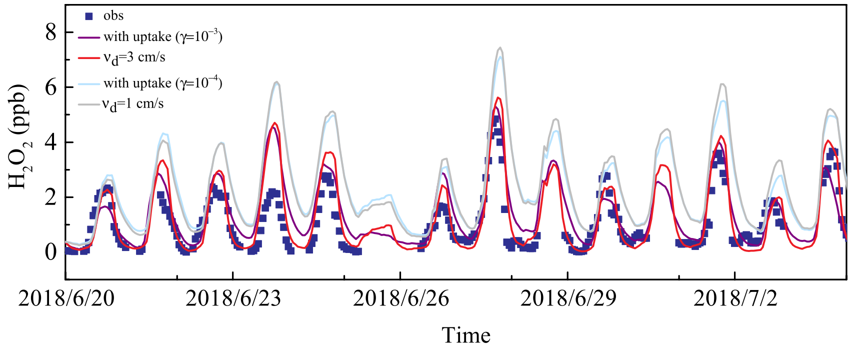

Figure 3. Observed and modeled H_2O_2 concentrations from June 20 to July 3, 2018 at the foot of Mt. Tai. The blue dots represent the measured concentrations. The red and gray lines represent the modeled results with dry deposition velocity of 3 and 1 cm s^{-1}, respectively. The purple and light blue lines represent modeled results with uptake coefficient of 1×10^{-3} and 1×10^{-4}, respectively.

3.4. The Sources and Sinks for H_2O_2

To disclose the reason for the relatively high atmospheric H_2O_2 concentration at the foot of Mt. Tai, a box model based on the Master Chemical Mechanism (MCM Version 3.3.1) was employed for preliminarily exploring the sources and sinks of the H_2O_2. In the initial running, H_2O_2 dry deposition velocity was set as 1 cm s^{-1} which was commonly used in box model simulations (Guo et al., 2014; Qin et al., 2018). As shown in Figure 3 (gray line), the modeling results could well reproduce the daily variation trend of H_2O_2, but both the H_2O_2 peak values in the daytime and minimal values at night were significantly overestimated ($H_2O_{2\ \mathrm{modeled}}/H_2O_{2\ \mathrm{measured}} = 1.8$), indicating that the sink for H_2O_2 might be largely underestimated. Some laboratory studies found that heterogeneous uptake by particles could be a sink for H_2O_2 (Pradhan et al., 2010; Romanias et al., 2012; Zhao et al., 2011). If the uptake coefficient of 1×10^{-4} was considered, H_2O_2 concentrations throughout the whole period were overestimated (light blue line in Figure 3). When the upper limit of H_2O_2 uptake coefficients (10^{-5}–10^{-3}) by particles derived from lab experiments were adopted (Pradhan et al., 2010; Romanias et al., 2012; Zhao et al., 2011), however, the simulated H_2O_2 concentrations were still overestimated especially during nighttime (the purple line in Figure 3). If the dry deposition velocity of 1 cm s^{-1} in the model was replaced by 3 cm s^{-1}, good agreement between the modeled and measured H_2O_2 could be achieved (the red line in Figure 3). The fast H_2O_2 dry deposition loss at the foot of Mt. Tai could be reflected by the high first-order decay rate constant ($k_d = 6 \times 10^{-5}\ s^{-1}$) of H_2O_2, which was derived by fitting the exponential decay curve (Figure S5) to the hourly averaged H_2O_2 concentrations from 19:00 to 6:00 according to the following equation:

$$k_d = \frac{\ln C_0 - \ln C}{t}$$

where, C_0 is the H_2O_2 concentration at $t = 0$ s, while C is the H_2O_2 concentration at t, and the slope of the linear regression of ($\ln C_0 - \ln C$) versus time t represents k_d.

Because the possible sinks of atmospheric H_2O_2 through photochemical reactions (e.g., the photolysis of H_2O_2 and its reaction with OH radicals) ceased at night, the H_2O_2 decay during the selected period was mainly ascribed to dry deposition. Then the dry deposition velocity (υ_d in unit of cm s^{-1}) of H_2O_2 could be estimated according to the following equation (Shepson et al., 1992):

$$\upsilon_d = k_d \times \mathrm{BLH}$$

Based on typical boundary layer heights (BLH) of 300–500 m at night in summer seasons (Tang et al., 2016; Zhu et al., 2018), υ_d value was estimated to be 1.8–3 cm s^{-1} which was in the range of 1–5 cm s^{-1} reported in previous studies (Crowley et al., 2018; Fischer et al., 2019; Hall & Claiborn, 1997; Liang et al., 2013; Nguyen et al., 2015), but higher than the commonly used value of 1 cm s^{-1} in model simulations. Additionally, the reactions of alkenes with O_3 also contributed to nighttime H_2O_2 at the foot, and thus the υ_d value obtained from the H_2O_2 decay at night in this study may only represent a lower limit of the H_2O_2 dry deposition velocity. Therefore, the upper υ_d value of 3 cm s^{-1} estimated might be reasonable for the model simulation,

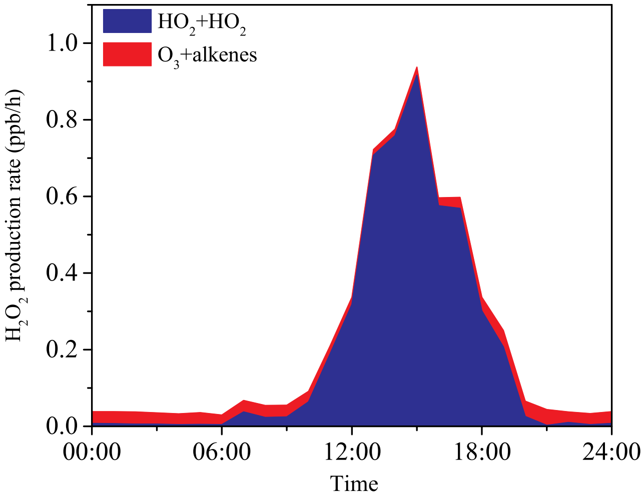

Figure 4. Modeled sources of H_2O_2 from June 20 to July 3, 2018.

resulting in the good agreement between the modeled and measured H_2O_2. Above results indicated H_2O_2 dry deposition velocity of 1 cm s^{-1} in box models might be underestimated. A recent study also suggested that 3D chemical transport models like GEOS-Chem model underestimated H_2O_2 dry deposition velocity which resulted in an enhancement of the simulated H_2O_2 surface concentrations by 45% (Nguyen et al., 2015). It should be pointed out that, however, the gas-phase model in our study did not consider the wet removal of H_2O_2 which may also bring some uncertainty to the dry deposition value. Nevertheless, the high dry deposition value estimated from our field measurements and modeling at least implied there existed a large sink of H_2O_2 near the ground at Tai'an city. Dry deposition velocity is closely related to the type of terrestrial surfaces and varies from site to site. Therefore, a fixed value may not be representative for one place to another. For example, higher dry deposition velocities were usually found in the forests (Hall & Claiborn 1997; Valverde-Canossa et al., 2006), where the underlying surface resistance is typically smaller. Uncertainties in the dry deposition velocity limit the simulations of H_2O_2 and its budget predictions in the troposphere. The need is high for more field observations to constrain the dry deposition parameterization and its input data to improve the use of air quality models for the public.

In addition to the self-combination of HO$_2$ radicals for H_2O_2 formation, the ozonolysis of alkenes has also been considered as an important source for atmospheric H_2O_2. This reaction produces Criegee intermediates, which then react with water vapor under atmospheric conditions yielding hydroxyalkyl hydroperoxides and subsequent decomposition leads to the formation of H_2O_2 (Valverde-Canossa et al., 2001). H_2O_2 production rates from the above two sources are illustrated in Figure 4. It is evident that the ozonolysis of alkenes acted as the dominant source for atmospheric H_2O_2 at night, whereas the self-combination of HO$_2$ accounted for more than 87% of the total production rate of H_2O_2 in the daytime. Three kinds of sinks for atmospheric H_2O_2 were considered in the model simulation: photolysis, reaction with OH radicals and dry deposition loss. The former two sinks only occur in the daytime, whereas the last one happens in both daytime and nighttime. Modeling results showed that H_2O_2 dry deposition was the dominant sink with a contribution of 84% to the total, followed by the reaction of H_2O_2 with OH (11%) and H_2O_2 photolysis (5%).

Atmospheric HO$_2$ radicals mainly come from the photooxidation processes of VOCs and CO, and thus a relative incremental reactivity (RIR) method (Cardelino & Chameides, 1995) was employed for exploring the relative contributions of VOCs species and CO to atmospheric H_2O_2. For a specific precursor of X, RIR$_X$ is defined as following formula:

$$\mathrm{RIR}_{(X)} = \frac{C\left(S_{(X)}\right) - C\left(S_{(X-\Delta X)}\right)}{C\left(S_{(X)}\right)}$$

where, $C(S_{(X)})$ represents the H_2O_2 concentration when its precursor concentration was $S(X)$, $C(S(X - \Delta X))$ represents the H_2O_2 concentration when its precursor concentration was reduced from $S(X)$ to $S(X - \Delta X)$.

In this study, the atmospheric concentrations of alkanes, alkenes, aromatics, HCHO, CH$_3$CHO, and CO were respectively reduced by 30% for exploring their relative contributions to atmospheric H_2O_2. As shown in Figure 5, the reduction of alkenes resulted in the highest RIR value of 0.223, followed by aromatics (0.125), HCHO (0.026), alkanes (0.017), CH$_3$CHO (0.008), and CO (−0.003). As alkenes and aromatics have higher photochemical reactivities relative to other VOC species, reduction of alkenes and aromatics lead to the more pronounced decrease of H_2O_2. Additionally, because of the double-bonded carbon atoms in alkene

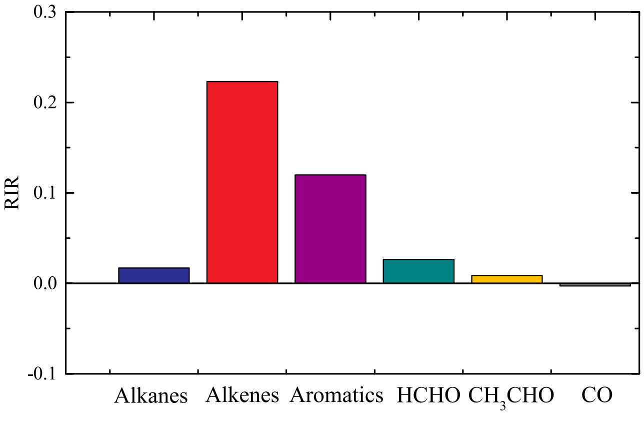

Figure 5. Sensitivity of H_2O_2 production to major VOC precursor groups, individual OVOC species and CO.

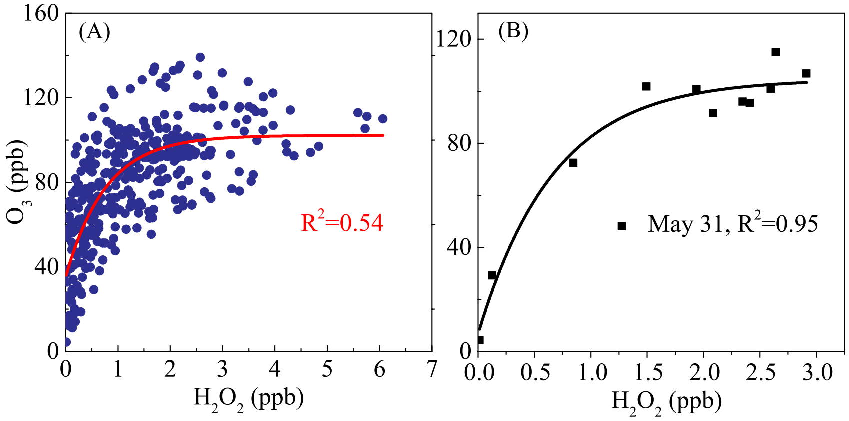

Figure 6. Correlation between hourly averaged H_2O_2 and O_3 concentrations from 8:00 to 18:00. (a) The period from May 30 to July 15, 2018. (b) Day on May 31.

molecules, they will also react with O_3 and NO_3 radical to produce HO_x radicals and subsequent H_2O_2 formation (Becker et al., 1993). Although the reaction of CO with OH produces HO_2 radicals, the OH consumption by atmospheric CO may slightly suppress the photochemical reactions of VOCs leading to less overall HO_2 production. Besides the formation of HO_2 radicals from the direct reactions of VOCs with OH, additional HO_2 can be produced through photolysis of the major products of carbonyls from the reactions, and thus CO reduction resulted in a small negative value of RIR. The large difference of RIR values among the VOCs species or classified compounds was mainly ascribed to their different photochemical reactivities. Although alkanes were the most abundant species, their reaction rate constants with OH radicals are usually 1–3 magnitudes slower than those of alkenes and aromatics (Atkinson et al., 2001), resulting in relatively small RIR values. The reaction rate constant of CH_3CHO (1.5×10^{-11} cm^3 molecule^{-1} s^{-1}) with OH radicals was nearly twice as that of HCHO (8.5×10^{-12} cm^3 molecule^{-1} s^{-1}) at 298 K (Atkinson et al., 2001), but the RIR value of HCHO was about a factor of 3 greater than that of CH_3CHO. Besides the OH-initiated reactions, photolysis of the aldehydes is also an important source for HO_2 radicals, for example, the photolysis of HCHO can produce fragments of H and HCO which readily react with O_2 to form two HO_2 radicals (Bufalini et al., 1972). Because the photolysis rate of HCHO is usually at least one magnitude greater than that of CH_3CHO under sunlight irradiation (Pang & Mu, 2006), the relatively high RIR for HCHO indicated its photolysis made a significant contribution to atmospheric HO_2 radicals. On the other hand, the HO_2 radicals formed from HCHO photolysis will partially be involved in the reaction with NO in polluted areas to recycle OH radicals which further initiate VOCs oxidation for more HO_2 formation.

As the photochemical reactions of VOCs initiated by OH radicals play key roles in H_2O_2 formation, the OH primary sources at the foot of Mt. Tai were also investigated by modeling calculations. O_3 and HONO are direct contributors to OH radicals. Since HCHO photolysis leads to HO_2 production and subsequent reaction with NO also yields OH radicals, O_3, HONO, and HCHO were all taken into consideration. As shown in Figure S6, the photolysis of O_3 was the dominant source for OH radicals, with a maximal OH production rate of 3.37 ppb h^{-1} at noontime, followed by photolysis of HCHO (2.91 ppb h^{-1}) and HONO (1.35 ppb h^{-1}).

Taking both the RIR values for the individual species and OH sources into account, the most efficient control measures for mitigating the H_2O_2 level at the ground site are the reduction of alkenes, aromatics and O_3 concentrations. Alkenes and aromatics reduction can be easily achieved through reducing their emission sources, but the reduction of O_3 should first assess the sensitive chemistry of O_3 formation which has a non-linear correlation with its precursors of VOCs and NO_x.

3.5. The Sensitive Chemistry for O_3 Formation

To explore the sensitive chemistry for O_3 formation at the ground site, the correlation between hourly averaged H_2O_2 and O_3 concentrations from 8:00 to 18:00 measured during the whole observation period and in a typical clear day are illustrated in Figure 6. When H_2O_2 was below 0.5 ppb, which mainly occurred in

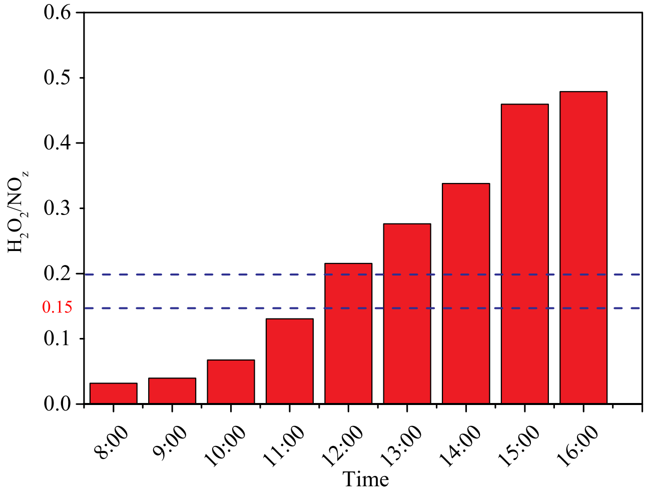

Figure 7. Average diurnal pattern of H_2O_2/NO_z ratio from 8:00 to 16:00 during the whole period.

the early morning hours, O_3 mixing ratio steeply increased with slight H_2O_2 elevation and $\Delta O_3/\Delta H_2O_2$ was usually >80, indicating that most of the HO_2 radicals formed from photochemical reactions of VOCs were involved in the conversion of NO to NO_2 and then generated O_3, namely O_3 formation is sensitive to VOCs. Whereas when H_2O_2 was greater than 1 ppb, which mainly appeared in the early afternoon, O_3 mixing ratio slowly increased or even remained constant with significantly increasing H_2O_2, revealing that most of the HO_2 radicals were involved in H_2O_2 formation through their recombination channel, that is, O_3 formation was sensitive to NO_x.

To further verify the above conclusions about O_3 sensitive chemistry, the average H_2O_2/NO_z ratios during daytime were also analyzed, which are illustrated in Figure 7. Like the H_2O_2/HNO_3 ratio, H_2O_2/NO_z ratio is also widely used as an indicator for diagnosing the VOCs-NO_x-O_3 sensitive chemistry (Castell et al., 2009; Reeves & Penkett, 2003; Sillman, 1995). NO_z is the sum of reactive nitrogen compounds which are the products from atmospheric conversion of NO_x, including HNO_3, nitrous acid (HONO), peroxyacetyl nitrates (PAN), organic nitrates, etc. In this study, the threshold values of $H_2O_2/NO_z = 0.15$–0.20 which are derived from model simulations (Sillman, 1995; Sillman et al., 1995, 1998), are adopted for judging the VOCs-NO_x-O_3 sensitive chemistry, that is,: the H_2O_2/NO_z ratios below, above and within the threshold values represent a VOC-sensitive regime, a NO_x-sensitive regime and a transition regime, respectively. The ratio was below 0.15 from 8:00 to 11:00 and above 0.2 from 12:00 to 16:00, implying that O_3 formation in Taian city was sensitive to VOCs in the morning hours and switched to NO_x-sensitive around noontime. The above-mentioned results are also consistent with other observations. For example, measured H_2O_2 concentrations in our study are comparable with those measured in other sites that are found to be mainly NO_x-sensitive, such as in Nashville, Tennessee (Weinstein-Lloyd et al., 1998). In addition, the measured H_2O_2 concentrations are much higher than those measured in locations which are believed to be mainly VOC-sensitive, like in Beijing city (He et al., 2010).

4. Conclusions

In this study, atmospheric H_2O_2 mixing ratios were measured at the foot of Mt. Tai in the summer of 2018 and at the summit of Mt. Tai in the summer of 2019, with average values of 0.93 ± 1.01 and 2.05 ± 1.20 ppb, respectively. The significantly high H_2O_2 levels in Tai'an city in comparison with the cities at approximately the same middle latitude implied that the photochemical pollution in the city is very serious. Compared with the measurements in summer of 2007, the remarkable elevation of H_2O_2 at the summit of Mt. Tai might be ascribed to VOCs increase and SO_2 decline in recent years. H_2O_2 exhibited a pronounced diurnal variation and reverse pattern with NO levels at the foot of Mt. Tai. With H_2O_2 dry deposition velocity of 3 cm s^{-1} included, the observed H_2O_2 concentrations at the foot of Mt. Tai could be well reproduced by a gas-phase box model, indicating H_2O_2 was mainly photochemically produced. Modeling analysis showed that the source and sink of H_2O_2 were dominated by HO_2 recombination and dry deposition loss, respectively. H_2O_2 production at the foot was found to be most sensitive to alkenes and aromatics by sensitivity tests, which demonstrated reducing alkenes and aromatics emissions were most efficient to decrease H_2O_2 concentrations. The evaluation of sensitive chemistry of O_3 in Tai'an city well elucidated that O_3 formation was VOC-sensitive in the early morning and shifted to NO_x-sensitive thereafter. Therefore, reduction of VOCs emissions especially for the reactive species of alkenes and aromatics in the morning as well as NO_x emissions around noontime will be effective for mitigating the serious O_3 (as well as H_2O_2) pollution in Tai'an city.

Data Availability Statement

Observation data are available at https://zenodo.org/record/5082201#.YObll8gufX8.

Acknowledgments

The authors thank Dr. Yunqiao Zhou for support in map plotting and Huan Song and Xiang Peng for helpful discussions. This work was supported by the National Natural Science Foundation of China (No. 91544211, 41727805, 41575121, 21707151), the National Research Program for Key issues in air pollution control (DQGG0103, DQGG0209, DQGG0206), and the National Key Research and Development Program of China (2016YFC0202200, 2017YFC0209703, 2017YFF0108301).

References

Anastasio, C., Faust, B. C., & Allen, J. M. (1994). Aqueous phase photochemical formation of hydrogen peroxide in authentic cloud waters. *Journal of Geophysical Research*, *99*(D4), 8231–8248. https://doi.org/10.1029/94jd00085

Atkinson, R., Baulch, D., Cox, R., Crowley, J., Hampson, R., Jr., Kerr, J., et al. (2001). Summary of evaluated kinetic and photochemical data for atmospheric chemistry. In: IUPAC subcommittee on gas kinetic data evaluation for atmospheric chemistry (20).

Balasubramanian, R., & Husain, L. (1997). Observations of gas-phase hydrogen peroxide at an elevated rural site in New York. *Journal of Geophysical Research*, *102*(D17), 21209–21220. https://doi.org/10.1029/97jd01480

Becker, K. H., Bechara, J., & Brockmann, K. (1993). Studies on the formation of H_2O_2 in the ozonolysis of alkenes. *Atmospheric Environment. Part A. General Topics*, *27*(1), 57–61. https://doi.org/10.1016/0960-1686(93)90070-f

Becker, K. H., Brockmann, K. J., & Bechara, J. (1990). Production of hydrogen peroxide in forest air by reaction of ozone with terpenes. *Nature*, *346*(6281), 256–258. https://doi.org/10.1038/346256a0

Bufalini, J. J., Gay, B. W., Jr., & Brubaker, K. L. (1972). Hydrogen peroxide formation from formaldehyde photooxidation and its presence in urban atmospheres. *Environmental Science & Technology*, *6*(9), 816–821. https://doi.org/10.1021/es60068a005

Calvert, J. G., Lazrus, A., Kok, G. L., Heikes, B. G., Walega, J. G., Lind, J., & Cantrell, C. A. (1985), Chemical mechanisms of acid generation in the troposphere, *Nature*, *317*(6032), 27–35. https://doi.org/10.1038/317027a0

Cardelino, C. A., & Chameides, W. L. (1995). An observation-based model for analyzing ozone precursor relationships in the urban atmosphere. *Journal of the Air & Waste Management Association*, *45*(3), 161–180. https://doi.org/10.1080/10473289.1995.10467356

Castell, N., Stein, A. F., Mantilla, E., Salvador, R., & Millán, M. (2009). Evaluation of the use of photochemical indicators to assess ozone—NO_X—VOC sensitivity in the Southwestern Iberian Peninsula. *Journal of Atmospheric Chemistry*, *63*(1), 73–91. https://doi.org/10.1007/s10874-010-9158-x

Claiborn, C. S., & Aneja, V. P. (1991). Measurements of atmospheric hydrogen peroxide in the gas phase and in cloud water at Mt. Mitchell, North Carolina. *Journal of Geophysical Research: Atmospheres*, *96*(D10), 18771–18787. https://doi.org/10.1029/91jd00931

Crowley, J. N., Pouvesle, N., Phillips, G. J., Axinte, R., Fischer, H., Petäjä, T., et al. (2018). Insights into HOx and ROx chemistry in the boreal forest via measurement of peroxyacetic acid, peroxyacetic nitric anhydride (PAN) and hydrogen peroxide. *Atmospheric Chemistry and Physics*. *18*(18).

Cui, Y., Yin, Y., Chen, K., Zhang, X., Kuang, X., Jiang, H., et al. (2020). Characteristics and sources of WSI in North China Plain: A simultaneous measurement at the summit and foot of Mount Tai. *Journal of Environmental Sciences*, *92*, 264–277. https://doi.org/10.1016/j.jes.2020.02.017

de Reus, M., Fischer, H., Sander, R., Gros, V., Kormann, R., Salisbury, G., et al. (2005). Observations and model calculations of trace gas scavenging in a dense Saharan dust plume during MINATROC. *Atmospheric Chemistry and Physics*, *5*(7), 1787–1803. https://doi.org/10.5194/acp-5-1787-2005

Ding, A. J., Wang, T., Thouret, V., Cammas, J. P., & Nedelec, P. (2008). Tropospheric ozone climatology over Beijing: Analysis of aircraft data from the MOZAIC program. *Atmospheric Chemistry and Physics*, *8*(1), 1–13. https://doi.org/10.5194/acp-8-1-2008

Faust, B. C., Anastasio, C., Allen, J. M., & Arakaki, T. (1993). Aqueous-phase photochemical formation of peroxides in authentic cloud and fog waters. *Science*, *260*(5104), 73–75. https://doi.org/10.1126/science.8465202

Fischer, H., Axinte, R., Bozem, H., Crowley, J. N., Ernest, C., Gilge, S., et al. (2019). Diurnal variability, photochemical production and loss processes of hydrogen peroxide in the boundary layer over Europe. *Atmospheric Chemistry and Physics*, *19*(18), 11953–11968. https://doi.org/10.5194/acp-19-11953-2019

Fischer, H., Pozzer, A., Schmitt, T., Jöckel, P., Klippel, T., Taraborrelli, D., & Lelieveld, J. (2015). Hydrogen peroxide in the marine boundary layer over the South Atlantic during the OOMPH cruise in March 2007. *Atmospheric Chemistry and Physics*, *15*(12), 6971–6980. https://doi.org/10.5194/acp-15-6971-2015

Gao, J., Wang, T., Ding, A. J., & Liu, C. B. (2005). Observational study of ozone and carbon monoxide at the summit of mount Tai (1534 m a.s.l.) in central-eastern China. *Atmospheric Environment*, *39*(26), 4779–4791. https://doi.org/10.1016/j.atmosenv.2005.04.030

Geng, G. N., Xiao, Q. Y., Zheng, Y. X., Tong, D., Zhang, Y. X., Zhang, X. Y., et al. (2019). Impact of China's air pollution prevention and control action plan on $PM_{2.5}$ chemical composition over eastern China. *Science China Earth Sciences*, *62*(12), 1872–1884. https://doi.org/10.1007/s11430-018-9353-x

Gong, Y., Xu, X., Xu, W., & Zhang, G. (2018). Characteristics of atmospheric hydrogen peroxide at an urban site in Beijing during winter and spring. *Journal of Meteorological Science*, *29*(4), 474–486.

Guo, J., Tilgner, A., Yeung, C., Wang, Z., Louie, P. K. K., Luk, C. W. Y., et al. (2014). Atmospheric peroxides in a polluted subtropical environment: Seasonal variation, sources and sinks, and importance of heterogeneous processes. *Environmental Science & Technology*, *48*(3), 1443–1450. https://doi.org/10.1021/es403229x

Hall, B. D., & Claiborn, C. S. (1997). Measurements of the dry deposition of peroxides to a Canadian boreal forest. *Journal of Geophysical Research*, *102*(D24), 29343–29353. https://doi.org/10.1029/97jd01113

Hammer, M. U., Vogel, B., & Vogel, H. (2002). Findings on H_2O_2/HNO_3 as an indicator of ozone sensitivity in Baden-Württemberg, Berlin-Brandenburg, and the Po valley based on numerical simulations. *Journal of Geophysical Research*, *107*(D22). LOP 3-1–LOP 3-18. https://doi.org/10.1029/2000jd000211

He, S. Z., Chen, Z. M., Zhang, X., Zhao, Y., Huang, D. M., Zhao, J. N., et al. (2010). Measurement of atmospheric hydrogen peroxide and organic peroxides in Beijing before and during the 2008 Olympic Games: Chemical and physical factors influencing their concentrations. *Journal of Geophysical Research*, *115*, D1730710. https://doi.org/10.1029/2009jd013544

Heland, J., Kleffmann, J., Kurtenbach, R., & Wiesen, P. (2001). A new instrument to measure gaseous nitrous acid (HONO) in the atmosphere. *Environmental Science & Technology*, *35*(15), 3207–3212. https://doi.org/10.1021/es000303t

Herrmann, H., Schaefer, T., Tilgner, A., Styler, S. A., Weller, C., Teich, M., & Otto, T. (2015). Tropospheric aqueous-phase chemistry: Kinetics, mechanisms, and its coupling to a changing gas phase. *Chemical Review*, *115*, 4259–4334. https://doi.org/10.1021/cr500447k

Hua, W., Chen, Z. M., Jie, C. Y., Kondo, Y., Hofzumahaus, A., Takegawa, N., et al. (2008), Atmospheric hydrogen peroxide and organic hydroperoxides during PRIDE-PRD'06, China: Their concentration, formation mechanism and contribution to secondary aerosols, *Atmospheric Chemistry and Physics*, *8*(22), 6755–6773. https://doi.org/10.5194/acp-8-6755-2008

Kanaya, Y., Akimoto, H., Wang, Z., Pochanart, P., Kawamura, K., Liu, Y., et al. (2013). Overview of the Mount Tai experiment (MTX2006) in central East China in June 2006: Studies of significant regional air pollution. *Atmospheric Chemistry and Physics*. *13*(16). https://doi.org/10.5194/acp-13-8265-2013

Lazrus, A. L., Kok, G. L., Lind, J. A., Gitlin, S. N., Heikes, B. G., & Shetter, R. E. (1986), Automated fluorometric method for hydrogen-peroxide in air, *Analytical Chemistry*, *58*(3), 594–597, https://doi.org/10.1021/Ac00294a024

Lee, M., Heikes, B. G., Jacob, D. J., Sachse, G., & Anderson, B. (1997). Hydrogen peroxide, organic hydroperoxide, and formaldehyde as primary pollutants from biomass burning. *Journal of Geophysical Research*, *102*(D1), 1301–1309. https://doi.org/10.1029/96jd01709

Lee, M., Kie, J. A., Kim, Y. M., & Lee, G. (2008). Characteristics of atmospheric hydrogen peroxide variations in Seoul megacity during 2002–2004. *The Science of the Total Environment*, *393*(2–3), 299–308. https://doi.org/10.1016/j.scitotenv.2007.11.037

Li, J. R., Zhu, C., Chen, H., Fu, H. B., Xiao, H., Wang, X. F., et al. (2020). A more important role for the ozone-S(IV) oxidation pathway due to decreasing acidity in clouds. *Journal of Geophysical Research: Atmospheres*, *125*(18), e2020JD033220. https://doi.org/10.1029/2020jd033220

Liang, H., Chen, Z. M., Huang, D., Zhao, Y., & Li, Z. Y. (2013). Impacts of aerosols on the chemistry of atmospheric trace gases: A case study of peroxides and HO_2 radicals. *Atmospheric Chemistry and Physics*, *13*(22), 11259–11276. https://doi.org/10.5194/acp-13-11259-2013

Liu, C., Mu, Y., Zhang, C., Zhang, Z., Zhang, Y., Liu, J., et al. (2016). Development of gas chromatography-flame ionization detection system with a single column and liquid nitrogen-free for measuring atmospheric C2–C12 hydrocarbons. *Journal of Chromatography A*, *1427*, 134–141. https://doi.org/10.1016/j.chroma.2015.11.060

Liu, J., Steinberg, S. M., & Johnson, B. J. (2003). A high performance liquid chromatography method for determination of gas-phase hydrogen peroxide in ambient air using Fenton's chemistry. *Chemosphere*, *52*(5), 815–823. https://doi.org/10.1016/s0045-6535(03)00260-1

Liu, T., Clegg, S. L., & Abbatt, J. P. (2020). Fast oxidation of sulfur dioxide by hydrogen peroxide in deliquesced aerosol particles. *Proceedings of the National Academy of Sciences of the United Stated of America*, *117*(3), 1354–1359. https://doi.org/10.1073/pnas.1916401117

Möller, D. (1989). The possible role of H_2O_2 in new-type forest decline. *Atmospheric Environment*, *23*(7), 1625–1627. https://doi.org/10.1016/0004-6981(89)90430-7

Nguyen, T. B., Crounse, J. D., Teng, A. P., St Clair, J. M., Paulot, F., Wolfe, G. M., & Wennberg, P. O. (2015). Rapid deposition of oxidized biogenic compounds to a temperate forest. *Proceedings of the National Academy of Sciences of the United States of America*, *112*(5), E392–E401. https://doi.org/10.1073/pnas.1418702112

Nunnermacker, L. J., Weinstein-Lloyd, J. B., Hillery, B., Giebel, B., Kleinman, L. I., Springston, S. R., et al. (2008). Aircraft and ground-based measurements of hydroperoxides during the 2006 MILAGRO field campaign. *Atmospheric Chemistry and Physics*, *8*(24), 7619–7636. https://doi.org/10.5194/acp-8-7619-2008

O'Sullivan, D., Heikes, B., Lee, M., Chang, W., Gregory, G., Blake, D., & Sachse, G. (1999). Distribution of hydrogen peroxide and methylhydroperoxide over the Pacific and South Atlantic Oceans. *Journal of Geophysical Research*, *104*(D5), 5635–5646. https://doi.org/10.1029/98jd01250

Pang, X., & Mu, Y. (2006). Seasonal and diurnal variations of carbonyl compounds in Beijing ambient air. *Atmospheric Environment*, *40*(33), 6313–6320. https://doi.org/10.1016/j.atmosenv.2006.05.044

Peng, Y., Chen, K., Lai, C., Lu, P., & Kao, J. (2006). Concentrations of H_2O_2 and HNO_3 and O_3–VOC–NO_X sensitivity in ambient air in southern Taiwan. *Atmospheric Environment*, *40*(35), 6741–6751. https://doi.org/10.1016/j.atmosenv.2006.05.079

Penkett, S. A., Jones, B. M. R., Brice, K. A., & Eggleton, A. E. J. (1979). Importance of atmospheric ozone and hydrogen-peroxide in oxidizing sulfur-dioxide in cloud and rainwater. *Atmospheric Environment*, *13*(1), 123–137. https://doi.org/10.1016/0004-6981(79)90251-8

Pradhan, M., Kalberer, M., Griffiths, P. T., Braban, C. F., Pope, F. D., Cox, R. A., & Lambert, R. M. (2010). Uptake of gaseous hydrogen peroxide by submicrometer titanium dioxide aerosol as a function of relative humidity. *Environmental Science & Technology*, *44*(4), 1360–1365. https://doi.org/10.1021/es902916f

Qin, M., Chen, Z., Shen, H., Li, H., Wu, H., & Wang, Y. (2018). Impacts of heterogeneous reactions to atmospheric peroxides: Observations and budget analysis study. *Atmospheric Environment*, *183*, 144–153. https://doi.org/10.1016/j.atmosenv.2018.04.005

Reeves, C. E., & Penkett, S. A. (2003). Measurements of peroxides and what they tell us. *Chemical Reviews*, *103*(12), 5199–5218. https://doi.org/10.1021/cr0205053

Ren, Y., Ding, A., Wang, T., Shen, X., Guo, J., Zhang, J., et al. (2009). Measurement of gas-phase total peroxides at the summit of Mount Tai in China. *Atmospheric Environment*, *43*(9), 1702–1711. https://doi.org/10.1016/j.atmosenv.2008.12.020

Romanias, M. N., El Zein, A., & Bedjanian, Y. (2012). Heterogeneous interaction of H_2O_2 with TiO_2 surface under dark and UV light irradiation conditions. *The Journal of Physical Chemistry A*, *116*(31), 8191–8200. https://doi.org/10.1021/jp305366v

Sakugawa, H., & Kaplan, I. R. (1993). Comparison of H_2O_2 and O_3 content in atmospheric samples in the San Bernardino Mountains, Southern California *Atmospheric Environment. Part A. General Topics*, *27*(9), 1509–1515. https://doi.org/10.1016/0960-1686(93)90136-m

Sander, S., Friedl, R., Barker, J., Golden, D., Kurylo, M., Wine, P., et al. (2003). *Chemical kinetics and photochemical data for use in atmospheric studies, evaluation number 14* (25, p. 334). JPL Publishing.

Shen, X., Lee, T., Guo, J., Wang, X., Li, P., Xu, P., et al. (2012). Aqueous phase sulfate production in clouds in eastern China. *Atmospheric Environment*, *62*, 502–511. https://doi.org/10.1016/j.atmosenv.2012.07.079

Shepson, P., Bottenheim, J., Hastie, D., & Venkatram, A. (1992). Determination of the relative ozone and PAN deposition velocities at night. *Geophysical Research Letters*, *19*(11), 1121–1124. https://doi.org/10.1029/92gl01118

Sillman, S. (1995). The use of NO_y, H_2O_2, and HNO_3 as indicators for ozone-NO_x-hydrocarbon sensitivity in urban locations. *Journal of Geophysical Research*, *100*(D7), 14175–14188. https://doi.org/10.1029/94jd02953

Sillman, S., Al-Wali, K. I., Marsik, F. J., Nowacki, P., Samson, P. J., Rodgers, M. O., et al. (1995). Photochemistry of ozone formation in Atlanta, GA-Models and measurements. *Atmospheric Environment*, *29*(21), 3055–3066. https://doi.org/10.1016/1352-2310(95)00217-m

Sillman, S., He, D., Pippin, M. R., Daum, P. H., Imre, D. G., Kleinman, L. I., et al. (1998). Model correlations for ozone, reactive nitrogen, and peroxides for Nashville in comparison with measurements: Implications for O_3-NO_x-hydrocarbon chemistry. *Journal of Geophysical Research*, *103*(D17), 22629–22644. https://doi.org/10.1029/98jd00349

Sommariva, R., Cox, S., Martin, C., Borońska, K., Young, J., Jimack, P. K., et al. (2020). AtChem (version 1), an open-source box model for the master chemical mechanism. *Geoscientific Model Development*, *13*(1), 169–183. https://doi.org/10.5194/gmd-13-169-2020

Sun, L., Xue, L., Wang, T., Gao, J., Ding, A., Cooper, O. R., et al. (2016). Significant increase of summertime ozone at Mount Tai in Central Eastern China. *Atmospheric Chemistry and Physics*, *16*(16).

Tan, Z., Rohrer, F., Lu, K., Ma, X., Bohn, B., Broch, S., et al. (2018). Wintertime photochemistry in Beijing: Observations of RO_x radical concentrations in the North China Plain during the BEST-ONE campaign. *Atmospheric Chemistry and Physics*, *18*(16), 12391–12411. https://doi.org/10.5194/acp-18-12391-2018

Tang, G., Zhang, J., Zhu, X., Song, T., Münkel, C., Hu, B., et al. (2016). Mixing layer height and its implications for air pollution over Beijing, China. *Atmospheric Chemistry and Physics*, *16*(4), 2459–2475. https://doi.org/10.5194/acp-16-2459-2016

Tanner, R. L., & Schorran, D. E. (1995), Measurements of gaseous peroxides near the Grand-Canyon implication for summertime visibility impairment from aqueous-phase secondary sulfate formation, *Atmospheric Environment*, *29*(10), 1113–1122, https://doi.org/10.1016/1352-2310(95)00047-3

Tao, F., Gonzalez-Flecha, B., & Kobzik, L. (2003). Reactive oxygen species in pulmonary inflammation by ambient particulates. *Free Radical Biology and Medicine*, *35*(4), 327–340. https://doi.org/10.1016/s0891-5849(03)00280-6

Valverde-Canossa, J., Ganzeveld, L., Rappenglück, B., Steinbrecher, R., Klemm, O., Schuster, G., & Moortgat, G. (2006). First measurements of H_2O_2 and organic peroxides surface fluxes by the relaxed eddy-accumulation technique. *Atmospheric Environment*, *40*, 55–67. https://doi.org/10.1016/j.atmosenv.2006.03.038

Valverde-Canossa, J., Grossmann, D., Neeb, P., & Moortgat, G. (2001). *Ozonolysis of biogenic and anthropogenic alkenes as a relevant source of tropospheric H_2O_2 and organic hydroperoxides*.

Vermeuel, M. P., Novak, G. A., Alwe, H. D., Hughes, D. D., Kaleel, R., Dickens, A. F., et al. (2019). Sensitivity of ozone production to NO_X and VOC along the Lake Michigan Coastline. *Journal of Geophysical Research: Atmospheres*, *124*(20), 10989–11006. https://doi.org/10.1029/2019jd030842

Walker, S. J., Evans, M. J., Jackson, A. V., Steinbacher, M., Zellweger, C., & McQuaid, J. B. (2006), Processes controlling the concentration of hydroperoxides at Jungfraujoch Observatory, Switzerland, *Atmospheric Chemistry and Physics*, *6*, 5525–5536. https://doi.org/10.5194/acp-6-5525-2006

Wang, Y., Chen, Z., Wu, Q., Liang, H., Huang, L., Li, H., et al. (2016). Observation of atmospheric peroxides during Wangdu campaign 2014 at a rural site in the North China Plain. *Atmospheric Chemistry and Physics*, *16*(17), 10985–11000. https://doi.org/10.5194/acp-16-10985-2016

Watanabe, K., Ishizaka, Y., & Tanaka, H. (1995). Measurements of atmospheric peroxides concentrations near the summit of Mt. Norikura in Japan. *Journal of the Meteorological Society of Japan*, *73*(6), 1153–1160. https://doi.org/10.2151/jmsj1965.73.6_1153

Watanabe, K., Yachi, C., Nishibe, M., Michigami, S., Saito, Y., Eda, N., et al. (2016). Measurements of atmospheric hydroperoxides over a rural site in central Japan during summers using a helicopter. *Atmospheric Environment*, *146*, 174–182. https://doi.org/10.1016/j.atmosenv.2016.06.074

Weinstein-Lloyd, J., Lee, J., Daum, P., Kleinman, L., Nunnermacker, L., Springston, S., & Newman, L. (1998). Measurements of peroxides and related species during the 1995 summer intensive of the Southern Oxidants Study in Nashville, Tennessee. *Journal of Geophysical Research*, *103*(D17), 22361–22373.

Ye, C., Liu, P., Ma, Z., Xue, C., Zhang, C., Zhang, Y., et al. (2018). High H_2O_2 concentrations observed during haze periods during the winter in Beijing: Importance of H_2O_2 oxidation in sulfate hormation. *Environmental Science and Technology Letters*, *5*, 757–763. https://doi.org/10.1021/acs.estlett.8b00579

Zhang, Q., Liu, J., He, Y., Yang, J., Gao, J., Liu, H., et al. (2018). Measurement of hydrogen peroxide and organic hydroperoxide concentrations during autumn in Beijing, China. *Journal of Environmental Sciences*, *64*, 72–81. https://doi.org/10.1016/j.jes.2016.12.015

Zhang, Q., Yuan, B., Shao, M., Wang, X., Lu, S., Lu, K., et al. (2014). Variations of ground-level O_3 and its precursors in Beijing in summertime between 2005 and 2011. *Atmospheric Chemistry and Physics*, *14*(12), 6089–6101. https://doi.org/10.5194/acp-14-6089-2014

Zhao, Y., Chen, Z., Shen, X., & Zhang, X. (2011). Kinetics and mechanisms of heterogeneous reaction of gaseous hydrogen peroxide on mineral oxide particles. *Environmental Science & Technology*, *45*(8), 3317–3324. https://doi.org/10.1021/es104107c

Zhou, L. H., Zhang, J., Zheng, X. H., Xue, W. H., & Zhu, S. G. (2019). Impacts of chemical and synoptic processes on summer tropospheric ozone trend in North China. *Advances in Meteorology*, *2019*, 3148432. https://doi.org/10.1155/2019/3148432

Zhu, X., Tang, G., Guo, J., Hu, B., Song, T., Wang, L., et al. (2018). Mixing layer height on the North China Plain and meteorological evidence of serious air pollution in southern Hebei. *Atmospheric Chemistry and Physics*, *18*(7), 4897–4910. https://doi.org/10.5194/acp-18-4897-2018

Zuo, Y., & Hoigné, J. (1993). Evidence for photochemical formation of H_2O_2 and oxidation of SO_2 in authentic fog water. *Science*, *260*(5104), 71–73. https://doi.org/10.1126/science.260.5104.71